RECENT UPGRADES AND TESTING THE OPTICAL SYSTEM OF THE 35 CM TELESCOPE AT THE STUDENTS ASTRONOMICAL OBSERVATORY „PLANA"

ANTONIYA VALCHEVA[1], PENCHO MARKISHKI[2], MILEN MINEV[1], ANDON KOSTOV[2], GANTCHO GANTCHEV[1], EVGENI OVCHAROV[1], PETKO NEDIALKOV[1]

[1] *Department of Astronomy,*
[2] *Institute of Astronomy with NAO Rozhen, BAS*

Антония Вълчева, Пенчо Маркишки, Милен Минев, Андон Костов, Ганчо Ганчев, Евгени Овчаров, Петко Недялков. ПОСЛЕДНИ ПОДОБРЕНИЯ И ТЕСТВАНЕ НА ОПТИЧНАТА СИСТЕМА НА 35 СМ ТЕЛЕСКОП В СТУДЕНТСКАТА АСТРОНОМИЧЕСКА ОБСЕРВАТОРИЯ „ПЛАНА"

Оптичната система на 35 cm (350/1600) телескоп на катедра „Астрономия", монтиран в Студентската астрономическа обсерватория „Плана", беше модернизирана. Вторичното огледало бе заменено, с цел да се минимизират ефектите от винетирането на полето. Бе монтиран нов автоматичен фокусер за бързо и фино фокусиране на звездния профил. Качеството на звездните изображения и дълбочината на звездната фотометрия, получени с подобрената система, е оценено и резултатите са представени тук.

Antoniya Valcheva, Pencho Markishki, Milen Minev, Andon Kostov, Gantcho Gantchev, Evgeni Ovcharov, Petko Nedialkov. RECENT UPGRADES AND TESTING THE OPTICAL SYSTEM OF THE 35 CM TELESCOPE AT THE STUDENTS ASTRONOMICAL OBSERVATORY „PLANA"

The optical system of the 35 cm (350/1600) telescope of the Department of Astronomy, situated at the Students Astronomical Observatory „Plana" has been upgraded. The secondary mirror was replaced to minimize the effects of the vignetting on the images. A new automated focuser was mounted to fasten and precised focusing of the stellar profiles. The image quality and the photometry depth obtained with the upgraded system is gauged and presented here.

For contact: Antoniya Valcheva, Department of Astronomy, Faculty of Physics, University of Sofia „St. Kliment Ohridski", 5 J. Bourchier Blvd., 1164 Sofia, Bulgaria, Phone: +359 2 81 61 716, E-mail: valcheva@phys.uni-sofia.bg

1. INTRODUCTION: THE OPTICAL SYSTEM OF THE 35 CM TELESCOPE AT SAO „PLANA" AND IMAGE VIGNETTING

The Department of Astronomy at the University of Sofia „St. Kliment Ohridski" has at its disposal a 35 cm Newtonian telescope VX 14" Orion Optics, positioned at the Students Astronomical Observatory „Plana" (SAO „Plana"). Its optical parameters are described in [1].

In general, the vignetting effect is a gradual darkening of the image towards its edges, i.e. part of the incoming light is reduced by objects intruding into the light path. Schematically, the vignetting from a diaphragm is explained in Fig. 1, where r_{mir} is the radius of the primary mirror; d is the distance from the sensor to the diaphragm; f is the focal length of the primary mirror.

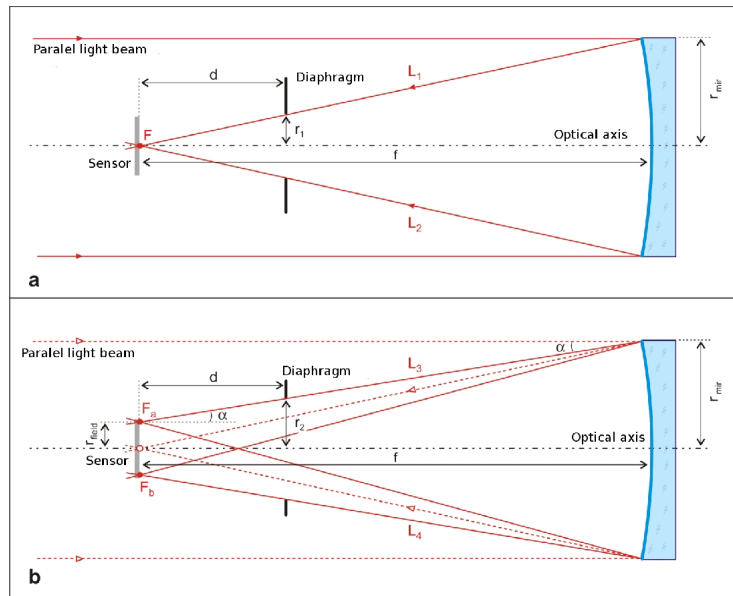**Fig. 1.** a) Scheme of the vignetting caused by a diaphragm with radius r_1; b) scheme of the reduced vignetting using a diaphragm with radius r_2 where $r_1 < r_2$

Case A: L_1 and L_2 are parallel rays focused on the main focus F (see Fig. 1a). In radius r_1 (the radius of the diaphragm) the entire convergent beam reflected from the primary mirror is focusing only in the main focus F. For all other points on the surface of the sensor (i.e. away from F) only part of the flux reaches it, since the surface is partially shaded (vignetted):

$$r_1 = d * r_{mir} / f \qquad (1)$$

Case B: Reduction of the vignetting can be made by increasing the diameter of the diaphragm as it is shown in Fig. 1b, where r_2 is the radius of the diaphragm; r_{field} is the radius of the vignetting-free field on the sensor; F_a and F_b are the images of two stars, being projected in two opposite ends of the vignetting-free field.

In order to prevent the convergent bundles from being partially shaded (i.e. the parallel rays L_3 and L_4 to also reach the focus), the radius r_2 of the diaphragm should be larger, as:

$$r_2 = r_{field} + (\tan\alpha * d), \quad \tan\alpha = (r_{mir} - r_{field})/f. \tag{2}$$

The vignetting is most prominent in the Newtonian telescopes and is mainly caused by the secondary mirror insufficient size or the focuser inside diameter, or both. So, if the vignetting is due to the insufficient size of the secondary mirror, then the minor axis of the secondary mirror should be enlarged as $2*r_2$, and the major axis $- (2*r_2)/\sin 45^o$.

The 35 cm telescope at SAO Plana is equipped with a secondary mirror with axes b/a = 82/116 mm and in its case, the central vignetting-free field, theoretically, should have a diameter of ~4 mm (445 pix), which is a small part of the image aria. This effect can be easily evaluated in the flat field profiles (the profiles of images taken on the sky after the sunset and before the dawn). In Fig. 2, top panels, the central BVR flat field profiles are shown and the vignetting-free central area has a diameter of ~600 pix and after that the relative flux starts to drop. Moreover, the central vertical profiles (the input boxes) show some misalignment in the optical components.
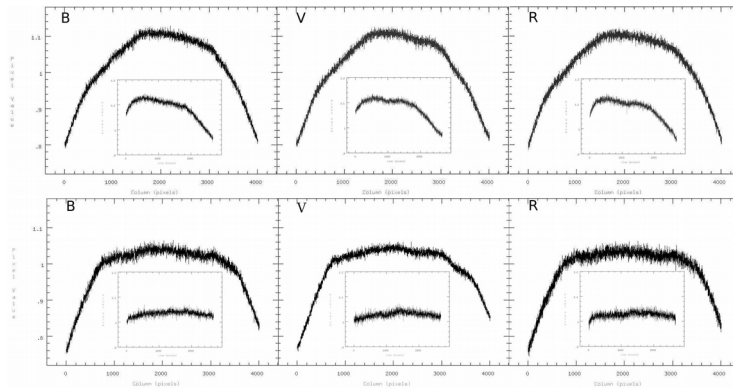

Fig. 2. Top: BVR central flat field profiles: horizontal profiles taken with the secondary elliptical b/a = 82/116 mm mirror and vertical profiles in the input boxes; Bottom: BVR central flat field profiles: horizontal profiles taken with the larger elliptical b/a = 100/141 mm mirror with the input vertical profiles

One of the main goal of this work is to increase the vignetting-free field and to prevent loosing part of the incoming light. As it was shown earlier, this can be achieved by increasing the size of the secondary mirror. The calculations show that to get the entire field free of vignetting, the secondary mirror should have a size b/a =112.3/158.8 mm. Unfortunately, the focuser diameter of 51 mm imposes a restriction and does not allow to achieve full-frame vignetting-free field. The reasonable maximal ratio of the secondary mirror is b/a = 92.7/131.1 mm. Mirror, offered by Orion Optics UK, with similar size is b/a =100/141 mm. In its case, the vignetting-free area on the image would have diameter of 18 mm (~2000 pix), which is nearly the short side of the CCD frame. This mirror was bought and mounted in the telescope tube.

Later on, the system was collimated and flat fields were taken. The central flat field profiles are shown in Fig. 2, bottom panels. The change is clearly visible. Now, the vignetting-free region can be evaluated to ~2500 pix (22.5 mm) in diameter. The profiles also allow us to test the mirrors collimation. The central vignetting-free aria in the horizontal profiles is well centered on the frame and the vertical profiles are flat as expected.

Another upgrade of the telescope, important for the telescope performance and for the observers, was also made. The existing manual focuser was replaced with Moonlite 2" short Crayford focuser with precise accessory locking and fine 1:8 dual speed transmission. This focuser is automated with MoonLite High Resolution Stepper Motor which works with MoonLite miniV2 controller and allows very precise, quick and automatic focusing of the system.

2. TESTING THE FIELD QUALITY

2.1. PERFORMANCE OF THE SYSTEM BEFORE THE UPGRADE

In order to test the full-frame image quality before the system upgrade, a set of images at different altitudes, i.e. different positions of the telescope tube according to the meridian flip were taken. The positions were ~70 deg in East and West direction and around zenith in East and West direction. During the observation campaign, the fields around M92 globular cluster and Vega star were observed with short exposures (30 and 60 sec) in R filter. The images were processed with IRAF (Image Reduction and Analysis Facility) and the finding algorithm searched for stellar objects in every observed field. Later, their individual FWHMs were obtained and the values of the measured FWHMs increase moving away from the center of the image. This effect is known as coma and is due to the blurring of the off-axis beams and creates a 'comet' like shape of the stellar images. The coma aberration is radial dependent, i.e. the minimum (fully focused) is around the central axis and increases towards the image edges. When the length of the coma exceeds the seeing of the image, the coma becomes noticeable and near the edges strongly distorts the stellar profiles. The addition of

a coma corrector would cause substantial reduction in the detected flux therefore it is preferable to use the central parts of the image without coma corrector and avoid the edges.

For every field, the stars were divided into 3 groups according to their FWHM — smaller than 3 pix (black dots), between [3−4] pix (gray filled circles) and between [4−5] pix (open circles), and the distributions of the groups over the image are shown in Fig. 3. The ellipses enclose the majority of the stars in a given FWHM interval and are drawn only to outline these distributions. Regardless the position of the telescope, the elliptical distribution is visible. This effect could probably be attributed to a perpendicular rotation at a small angle of the secondary mirror and also to its insufficient size. While the distributions in the zenith direction are probably due to some other displacements of the mirrors.
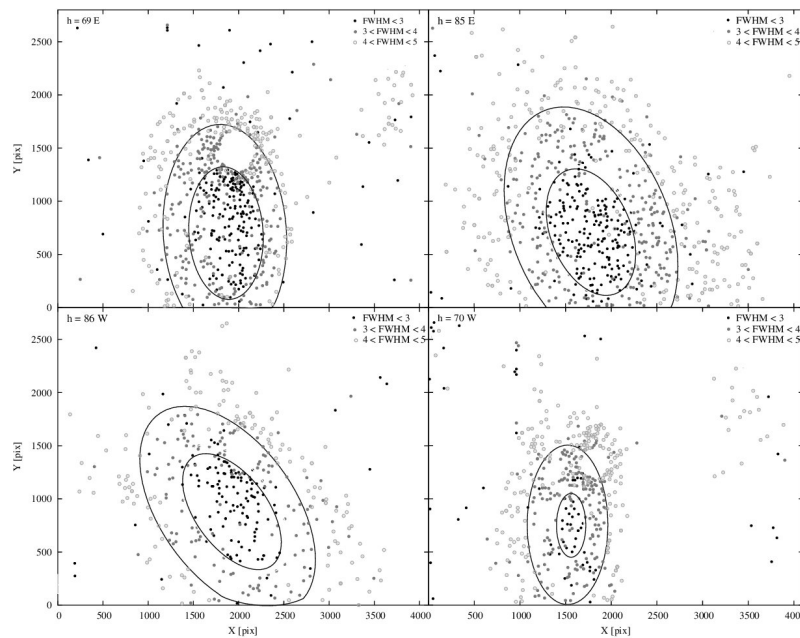

Fig. 3. Distribution of stars with FWHM in a given interval – less than 3 pix (black dots), between [3–4] pix (gray filled circles), and between [4−5] pix (open circles). The field of M92 cluster was observed at altitudes: 69 deg East (top left); 86 deg West (bottom left); and 70 deg West (bottom right). The field around Vega star was observed at 85 deg East. (The cited altitudes show the direction at which the object was observed thus the telescope tube was in the opposite direction according to the meridian flip.) The ellipses enclose the majority of the stars with a given FWHM and are used only to outline the distributions. The empty circle region close to the center of the frames is the core of M92 and the vicinity of Vega

After the secondary mirror and focuser replacement, test observations were made to study the collimation and the overall performance of the upgraded system. Random star fields were observed at 4 different positions of the telescope in East and West direction. The images were processed, all stellar objects were identified and their individual FWHMs were obtained. For every field, the stars were grouped according to their FWHM value − smaller than 3 pix (black dots), between [3−4] pix (gray filled circles) and between [4−5] pix (open circles) – and the groups distributions are shown in Fig. 4 and Fig. 5.

In Fig. 4, the results from the observations of random stellar fields in the eastern sky are presented and the telescope tube was on the West of the meridian flip. The altitudes of the observed fields are 55, 63, 78 and 90 deg. In Fig. 5 – the observed stellar fields were in the western sky and the telescope tube was on the East of the meridian flip. In both figures, circles are drown to outline the stars with FWHM in a given interval and one can see that FWHM distributions had nearly circular form and the stars with minimal FWHM can be found in the center of the image, without being affected by the position of the telescope.
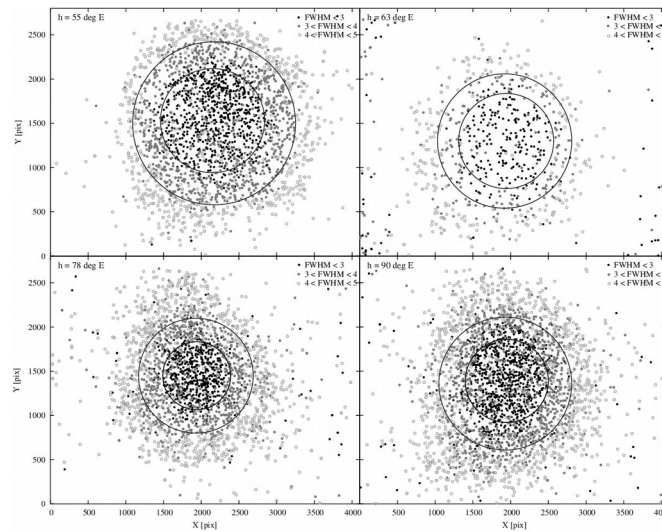

Fig. 4. Distribution of stars with FWHM in a given interval – less than 3 pix (black dots), between [3−4] pix (gray filled circles), and between [4−5] pix (open circles). Random stellar fields in East direction were observed at different altitudes – 55, 63, 78 and 90 deg − in order to test the performance of the optical system of the telescope after the upgrade. The circles enclose the majority of the stars with a given FWHM and are used only to outline the distributions

Despite the outwards stellar profile degradation which is due to the coma aberration, a circle aria with diameter nearly equal to the small side of the CCD frame can be certainly used, even in the cases with very good seeing conditions.
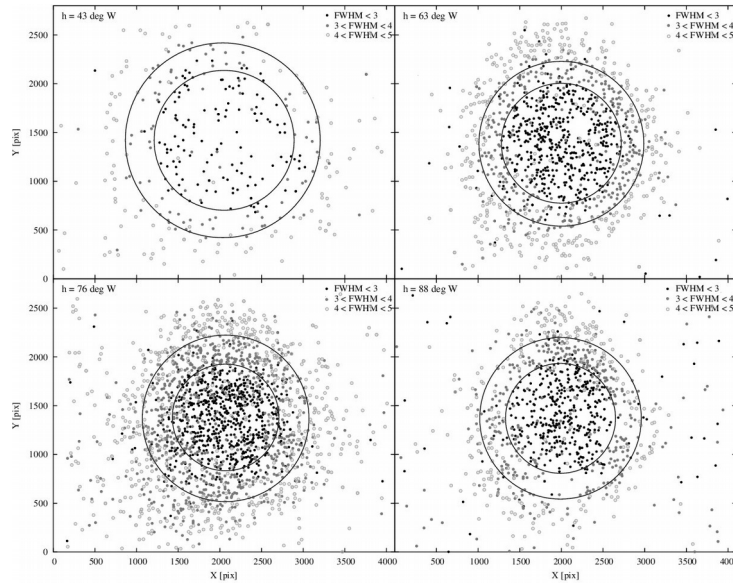

Fig. 5. Distribution of stars with FWHM in a given interval – less than 3 pix (black dots), between [3–4] pix (gray filled circles), and between [4–5] pix (open circles). Random stellar fields in West direction were observed at different altitudes – 43, 63, 76 and 88 deg – in order to test the performance of the optical system of the telescope after the upgrade. The circles enclose the majority of the stars with a given FWHM and are used only to outline the distributions

3. PHOTOMETRY DEPTH AND DATA QUALITY

To test the depth and the quality of the photometry after the telescope upgrade (see in [1] the test results obtained before the upgrade), we need standard stars to calibrate our instrumental magnitudes. For this purpose, the photometric standard fields of [2] are very suitable – they cover large areas and contain large number of stars. M92 globular cluster (NGC 6341) is one of the largest standard fields – 31'.4×27'.1 – and contains between 2000 and 4000 photometric standards in each UBVRI filters. We obtained 5×300 sec of M92 (see Fig. 6, left panel) in BVR filters. Calibration images – flat fields and dark currents – were also obtained.

After the initial reduction, the images in each filter were aligned and combined. Due to the high crowding, PSF photometry is required but in the case of variable FWHM (due to the coma aberration) a better approach is the aperture photometry. We excluded a circle area with radius ~2 arcmin centered on M92 to avoid strong star profiles overlapping. The atmospheric conditions were fairly good with seeing of ~3.2 arcsec. After DAOFIND/APPHOT have selected the objects in the field, the stars with FWHM larger than 2×<FWHM> (<FWHM> − the average FWHM in the central region) were excluded (these stars are highly affected by the coma). The PHOT/APPHOT task determined the instrumental magnitudes of the sources and finally we have 1736, 1760 and 1796 stars in B, V, and R filter, respectively. Their positions are shown in Fig. 6, right panel.
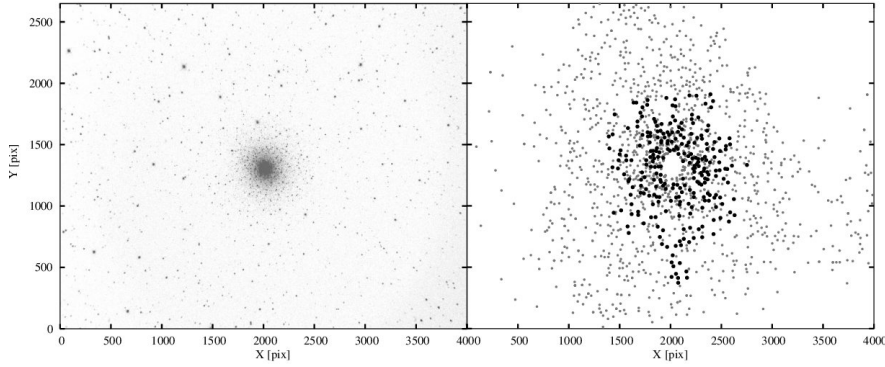

Fig. 6. Left: 78'×52' field around M92 globular cluster observed in R filter with the 35 cm telescope; Right: Positions of all stars with standard R magnitudes (small gray circles) and the cross-identified stars with [2] (black filled circles) are presented

To standardize our photometry, we needed to cross-identify our photometry with the standard stars of [2]; 228, 253, 130 stars were cross-identified in B, V and R filter, respectively, and the following transformation equations were found:

$$B = -4.243(\mp 0.004) + b$$
$$V = -4.567(\mp 0.005) + v$$
$$R = -4.875(\mp 0.005) + r$$

where b, v, r are the instrumental magnitudes and B, V and R are the standard magnitudes of the stars. Fig. 7 shows the standard magnitudes for stars with σ < 0.2 mag. Photometry with fairly good accuracy (σ < 0.05 mag) can be achieved up to ~18.3 mag in R (~18.5 mag in V; ~19 mag in B) and more than 19.5 mag with σ < 0.2 mag for the three filters.
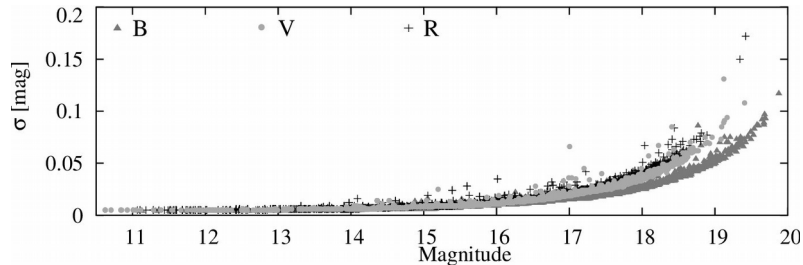
Fig. 7. Standard magnitudes versus uncertainties for *B* (triangle), *V* (circles) and *R* (crosses) filters. Only the stars with σ < 0.2 mag are plotted

4. CONCLUSIONS

The replacement of the secondary mirror of the 35 cm telescope at SAO „Plana" with bigger one led to minimization of the vignetting of the images taken with it. From flat fields central profiles was evaluated that the vignetting-free field increased from ~4 mm (445 pix) to ~22.5 mm (2500 pix) in diameter. The performance of the telescope and the image quality after the upgrade was tested by set of observations at different altitudes in East and West directions. Regardless the telescope tube position, the area with minimal FWHM is well centered on the image and the FWHM increased symmetrically from the center towards the edges. In all weather conditions, an area with diameter of ~2500 pix (small side of the CCD frame – 52 arcmin) can be used for science projects because the coma aberration effects are unessential.

The photometry depth was tested with 5×300 sec exposures in BVR filters and showed that magnitudes up to ~18.3 mag in *R* (~18.5 mag in *V*; ~19 mag in *B*) can be achieved with fairly good accuracy (σ < 0.05 mag) and deeper than 19.5 mag with σ < 0.2 mag for the three filters.

REFERENCES

[1] Ovcharov, E. et al. *BlgAJ*, 2014, 21, 19.
[2] Stetson, P. *PASP*, 2000, 112, 925.